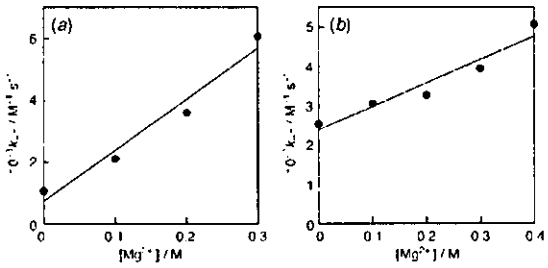

Fig. 1 Plots of k_{III} *vs.* $[Mg^{2+}]$ in the reaction of **III** with (a) DPPH$^{\cdot}$ and (b) GO$^{\cdot}$ in de-aerated MeOH at 298 K.

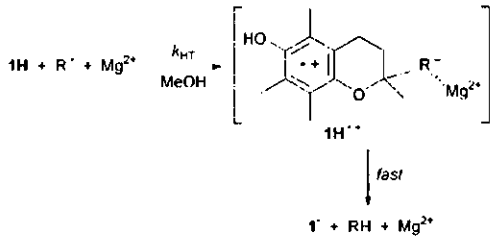

Scheme 1 Radical-scavenging reaction by **III** *via* an electron transfer in MeOH.

the coordination of Mg^{2+} to DPPH^{-} or GO^{-} may stabilize the product, resulting in the acceleration of the electron transfer.

Effect of base on the rates of radical scavenging reactions

In protic media, such as alcohols and water, **III** may be in equilibrium with the corresponding phenolate anion **I**$^{-}$, which is a much stronger electron donor as compared to the parent **III**.[20] In such a case, **I**$^{-}$ may act as an electron donor rather than the parent **III** in MeOH.

In order to clarify an actual electron donor in MeOH, the effect of base on the radical-scavenging rates of **III** was examined. The addition of pyridine to the **III**–DPPH$^{\cdot}$ system results in a significant increase in the rate of the DPPH$^{\cdot}$-scavenging reaction by **III**. The k_{III} value increases with increasing pyridine concentration to reach a constant value as shown in Fig. 2. When pyridine is replaced by 2,6-lutidine, a stronger base than pyridine, the limiting k_{III} value is larger than that in the case of pyridine, as shown in Fig. 2. If the rate of acceleration is due to the deprotonation of the phenolic OH group of **III** in the presence of base, the limiting k_{III} value should be the same regardless of the basicity of pyridines. The different limiting k_{III} values between pyridine and 2,6-lutidine in Fig. 2 suggest that little deprotonation occurs to produce **I**$^{-}$ and that the actual electron donor is the parent **III** rather than **I**$^{-}$ in MeOH, as shown in Scheme 1. In such a case, the coordination of pyridines

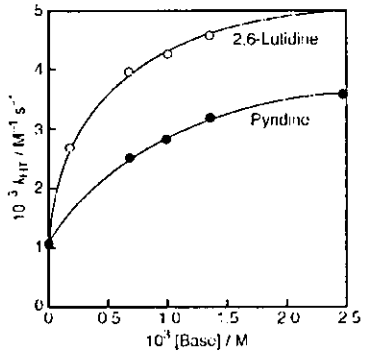

Fig. 2 Plot of k_{III} *vs.* [base] for the reaction of **III** with DPPH$^{\cdot}$ in the presence of pyridine (black circles) or 2,6-lutidine (white circles) in de-aerated MeOH at 298 K.

to **III**$^{+\cdot}$ may stabilize the product, resulting in the acceleration of the initial electron-transfer process. In the presence of a large amount of a strong Lewis acid, such as $Mg(ClO_4)_2$, no deprotonation of **III** occurs in MeOH.

Solvent effect on the one-electron oxidation potential of the vitamin E model

The solvent effect on the one-electron oxidation potential (E^{o}_{ox}) of **III** was examined by cyclic voltammetry (CV) and second-harmonic alternating current voltammetry (SHACV) measurements.[11,16] Very recently, Williams and Webster have reported that the one-electron oxidation of α-tocopherol itself occurs at about 0.97 V *vs.* SCE in MeCN (0.25 M Bu_4NPF_6) based on the detailed electrochemical analyses.[21] A similar cyclic voltammogram was observed for the electrochemical oxidation of **III** in MeCN (0.1 M Bu_4NClO_4) (data not shown), from which was determined the E^{o}_{ox} value (*vs.* SCE) of **III** in MeCN as 0.97 V. On the other hand, the CV wave of **III** in MeOH (0.1 M Bu_4NClO_4) was irreversible. Thus, SHACV measurement was carried out to determine the E^{o}_{ox} value of **III** in MeOH. The E^{o}_{ox} value (*vs.* SCE) of **III** in MeOH (0.1 M Bu_4NClO_4), determined from the intersection of an SHACV wave (Fig. 3), is located at 0.63 V, which is significantly more negative than the value in MeCN (0.97 V). Such a negative shift of the E^{o}_{ox} value in MeOH as compared to that in MeCN may be ascribed to a stronger solvation of **III**$^{+\cdot}$ in MeOH than in MeCN. Thus, the ease of one-electron oxidation of **III** in MeOH as compared to in MeCN may result in the difference in the radical-scavenging mechanism.

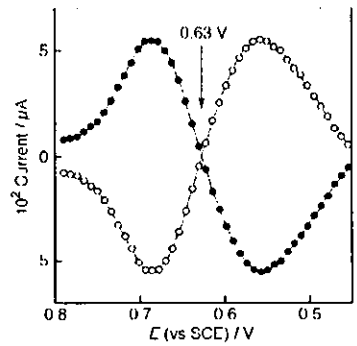

Fig. 3 SHACV of **III** recorded at the scan rate of 4 mV s^{-1} on Pt working electrode in de-aerated MeOH (0.1 M Bu_4NClO_4) at 298 K.

EPR spectrum of the phenoxyl radical derived from the vitamin E model in de-aerated MeOH

The EPR detection of radical species derived from **III** would provide valuable information about the solvation of the radical species.[22,23] The EPR spectrum of **I**$^{\cdot}$ in de-aerated MeOH at 298 K is shown in Fig. 4a. It should be noted that the *g* value of the EPR spectrum of **I**$^{\cdot}$ in MeOH (2.0040) is apparently smaller than that in MeCN (2.0047).[7] The observed hyperfine structure in Fig. 4a is well reproduced by the computer simulation (Fig. 4b) with four hyperfine splitting constants (*hfc*) listed in Table 1. Table 1 also shows the *hfc* values of **I**$^{\cdot}$ in MeCN.[7] All the *hfc* values in MeOH are also smaller than those in MeCN. The smaller *g* value of the EPR spectrum of **I**$^{\cdot}$ as well as the smaller *hfc* values in MeOH than those in MeCN indicates that the stronger solvation of **I**$^{\cdot}$ may occur in MeOH than in MeCN. Although the EPR spectrum of **III**$^{+\cdot}$ could not be observed because of the fast deprotonation to produce **I**$^{\cdot}$ (Scheme 1), stronger solvation of **III**$^{+\cdot}$ may also occur in MeOH than in MeCN, resulting in the ease of one-electron oxidation of **III** in MeOH than in MeCN.

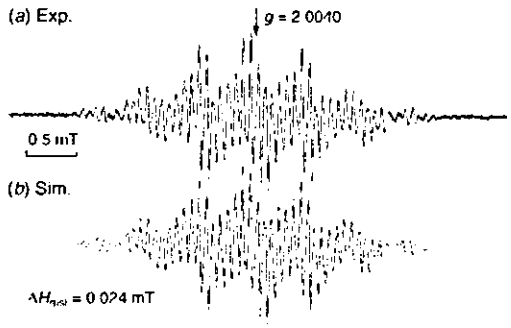

Fig. 4 (a) EPR spectrum of I$^{\bullet}$ generated in the reaction of **III** (1.0×10^{-3} M) with DPPH$^{\bullet}$ (2.0×10^{-3} M) in de-aerated MeOH at 298 K. (b) The computer simulation spectrum. The *hfc* values used for the simulation are listed in Table 1.

Table 1 Hyperfine splitting constants (*hfc*s in mT) and *g* values of I$^{\bullet}$ in de-aerated solvents

Solvent	*g*	*a*(3H$^{\alpha}$)	*a*(3H$^{\gamma}$)	*a*(3H$^{\gamma}$)	*a*(2H$^{\beta}$)
MeOH	2.0040	0.577	0.423	0.073	0.126
MeCN	2.0047[a]	0.587[a]	0.440[a]	0.086[a]	0.139[a]

[a] Taken from ref. 7.

In conclusion, the scavenging reaction of DPPH$^{\bullet}$ or GO$^{\bullet}$ by **III** in MeOH proceeds *via* the electron transfer from **III** to DPPH$^{\bullet}$ or GO$^{\bullet}$ followed by proton transfer rather than *via* the one-step hydrogen atom transfer, which has been observed in MeCN. Such a difference in the mechanism of radical-scavenging reactions by the vitamin E model depending on the solvents provides valuable information for the biological antioxidative reactions.

Acknowledgements

This work was partially supported by a Grant-in-Aid for Scientific Research (A) (No. 16205020) and a Grant-in-Aid for Young Scientist (B) (No. 15790032) from the Ministry of Education, Culture, Sports, Science and Technology, Japan.

References

1 J. S. Wright, E. R. Johnson and G. A. DiLabio, *J. Am. Chem. Soc.*, 2001, **123**, 1173.
2 M. Leopoldini, T. Marino, N. Russo and M. Toscano, *J. Phys. Chem. A*, 2004, **108**, 4916.
3 M. Leopoldini, I. P. Pitarch, N. Russo and M. Toscano, *J. Phys. Chem. A*, 2004, **108**, 92.
4 S. Fukuzumi, in *Electron Transfer in Chemistry*, ed. V. Balzani, Wiley-VCH, New York, 2001, vol. 4, pp. 3–67.
5 I. Nakanishi, K. Miyazaki, T. Shimada, K. Ohkubo, S. Urano, N. Ikota, T. Ozawa, S. Fukuzumi and K. Fukuhara, *J. Phys. Chem. A*, 2002, **106**, 11123.
6 I. Nakanishi, K. Ohkubo, K. Miyazaki, W. Hakamata, S. Urano, T. Ozawa, H. Okuda, S. Fukuzumi, N. Ikota and K. Fukuhara, *Chem. Res. Toxicol.*, 2004, **17**, 26.
7 I. Nakanishi, K. Fukuhara, T. Shimada, K. Ohkubo, Y. Iizuka, K. Inami, M. Mochizuki, S. Urano, S. Itoh, N. Miyata and S. Fukuzumi, *J. Chem. Soc., Perkin Trans. 2*, 2002, 1520.
8 I. Nakanishi, S. Matsumoto, K. Ohkubo, K. Fukuhara, H. Okuda, K. Inami, M. Mochizuki, T. Ozawa, S. Itoh, S. Fukuzumi and N. Ikota, *Bull. Chem. Soc. Jpn.*, 2004, **77**, 1741.
9 H.-Y. Zhang and L.-E. Wang, *J. Phys. Chem. A*, 2003, **107**, 11258.
10 D. D. Perrin, W. L. F. Armarego and D. R. Perrin, *Purification of Laboratory Chemicals, 4th Edition*, Pergamon Press, Elmsford, New York, 1996.
11 T. G. McCord and D. E. Smith, *Anal. Chem.*, 1969, **41**, 1423.
12 A. M. Bond and D. E. Smith, *Anal. Chem.*, 1974, **46**, 1946.
13 M. R. Wasielewski and R. Breslow, *J. Am. Chem. Soc.*, 1976, **98**, 4222.
14 E. M. Arnett, K. Amarnath, N. G. Harvey and J.-P. Cheng, *J. Am. Chem. Soc.*, 1990, **112**, 344.
15 M. Patz, H. Mayr, J. Maruta and S. Fukuzumi, *Angew. Chem., Int. Ed. Engl.*, 1995, **34**, 1225.
16 S. Fukuzumi, N. Satoh, T. Okamoto, K. Yasui, T. Suenobu, Y. Seko, M. Fujitsuka and O. Ito, *J. Am. Chem. Soc.*, 2001, **123**, 7756.
17 K. Mann and K. K. Barnes, in *Electrochemical Reactions in Nonaqueous Systems*, Marcel Dekker Inc., New York, 1990.
18 K. Mukai, Y. Watanabe and K. Ishizu, *Bull. Chem. Soc. Jpn.*, 1986, **59**, 2899.
19 G. Litwinienko and K. U. Ingold, *J. Org. Chem.*, 2003, **68**, 3433.
20 I. Nakanishi, K. Miyazaki, T. Shimada, Y. Iizuka, K. Inami, M. Mochizuki, S. Urano, H. Okuda, T. Ozawa, S. Fukuzumi, N. Ikota and K. Fukuhara, *Org. Biomol. Chem.*, 2003, **1**, 4085.
21 L. L. Williams and R. D. Webster, *J. Am. Chem. Soc.*, 2004, **126**, 12441.
22 T. Yonezawa, T. Kawamura, M. Ushio and Y. Nakao, *Bull. Chem. Soc. Jpn.*, 1970, **43**, 1022.
23 M. Lucarini, V. Mugnaini, G. F. Pedulli and M. Guerra, *J. Am. Chem. Soc.*, 2003, **125**, 8318.

EPR Study on Stable Magnesium Complexes of the Phenoxyl Radicals Derived from a Vitamin E Model and Its Deuterated Derivatives

Ikuo Nakanishi,*[1,2] Shigenobu Matsumoto,[3] Kei Ohkubo,[2] Kiyoshi Fukuhara,[4] Haruhiro Okuda,[4] Keiko Inami,[5] Masataka Mochizuki,[5] Toshihiko Ozawa,[1] Shinobu Itoh,[6] Shunichi Fukuzumi,*[2] and Nobuo Ikota*[1]

[1]Redox Regulation Research Group, Research Center for Radiation Safety, National Institute of Radiological Sciences, 4-9-1 Anagawa, Inage-ku, Chiba 263-8555

[2]Department of Material and Life Science, Graduate School of Engineering, Osaka University, CREST, Japan Science and Technology Agency, 2-1 Yamada-oka, Suita, Osaka 565-0871

[3]Tokyo Metropolitan Institute of Gerontology, 35-2 Sakae-cho, Itabashi-ku, Tokyo 173-0015

[4]Division of Organic Chemistry, National Institute of Health Sciences, 1-18-1 Setagaya-ku, Tokyo 158-8501

[5]Division of Organic and Bioorganic Chemistry, Kyoritsu College of Pharmacy, 1-5-30 Shibakoen, Minato-ku, Tokyo 105-8512

[6]Department of Chemistry, Graduate School of Science, Osaka City University, 3-3-138 Sugimoto, Sumiyoshi-ku, Osaka 558-8585

Received April 8, 2004; E-mail: nakanis@nirs.go.jp

The phenoxyl radical **1**•, generated by the reaction of a vitamin E model, 2,2,5,7,8-pentamethylchroman-6-ol (**1H**), with 2,2-bis(4-*tert*-octylphenyl)-1-picrylhydrazyl (DOPPH•), was significantly stabilized by complex formation with Mg^{2+} in deaerated acetonitrile at 298 K. The assignments of the hyperfine coupling constants (hfc) obtained by computer simulations of the observed EPR spectrum of the Mg^{2+} complex of **1**• (Mg^{2+}–**1**•), were carried out using three deuterated isotopomers of **1**•, i.e., 5-CD_3-**1**•, 7-CD_3-**1**•, and 8-CD_3-**1**•, where a methyl group at the C5, C7, or C8 position is replaced by a CD_3 group, respectively. The decreased spin density of the benzene ring in the Mg^{2+}–**1**• complex indicates that delocalization of the unpaired electron in **1**• into Mg^{2+} by complexation between Mg^{2+} and **1**• results in the enhanced stability of **1**• in the presence of Mg^{2+}.

Most biological antioxidants, such as vitamin E (α-tocopherol) and flavonoids, have one or more phenolic hydroxy groups, and are converted into phenoxyl radical intermediates as the result of antioxidative radical-scavenging reactions with active oxygen radicals, such as hydroxyl radical (•OH), superoxide anion ($O_2^{\bullet-}$), and lipid peroxyl radical (LOO•).[1–4] Thus, it is of great importance to detect and characterize the phenoxyl radicals of such antioxidants in order to shed light on the mechanism of the antioxidative radical-scavenging reactions in biological systems as well as to develop novel antioxidants with more effective antioxidative activities than the natural occurring ones. However, the phenoxyl radical of α-tocopherol is known to be unstable, because of disproportionation, even in the absence of molecular oxygen (O_2).[5] Furthermore, in the presence of O_2, a radical coupling between the phenoxyl radical derived from vitamin E and O_2 is known to produced a wide variety of oxidation products of the phenoxyl radical.[6–23] On the other hand, we have recently reported that the phenoxyl radical **1**• of a vitamin E model, 2,2,5,7,8-pentamethylchroman-6-ol (**1H**), generated by hydrogen transfer from **1H** to 2,2-bis(4-*tert*-octylphenyl)-1-picrylhydrazyl radical (DOPPH•) or galvinoxyl radical (G•), is significantly stabilized by the presence of Mg^{2+} via the complexation of **1**• with Mg^{2+}.[24] The well-resolved 14 lines were observed in the EPR spectrum of the Mg^{2+} complex of **1**• (Mg^{2+}–**1**•).[24] However, the hyperfine structure of the observed EPR spectrum of the Mg^{2+}–**1**• complex has yet to be sufficiently characterized, since there are three methyl groups in the **1**• molecule, each of which gives a quartet hyperfine coupling structure. On the other hand, it is known that deuterium substitution at appropriate known sites in the molecule permits an experimental verification of the assignment of the hyperfine coupling constants (hfc) for the EPR spectrum of the observed radical species.[25–29]

Here, we report on an experimental assignment of the hfc values of the EPR spectrum of the Mg^{2+} complex of **1**• using three deuterated isotopomers of **1**•, i.e., 5-CD_3-**1**•, 7-CD_3-**1**•, and 8-CD_3-**1**•, where a methyl group at the C5, C7, or C8 position is replaced by a CD_3 group, respectively (Chart 1). A comparison of the hfc values of the Mg^{2+}–**1**• complexes obtained in this study with those of the parent **1**• provides fundamental information about the spin distribution and stabilization of the phenoxyl radical species of phenolic antioxidants in the presence of metal ions, as well as mechanistic insight into the antioxidative radical-scavenging reactions of phenolic antioxidants.

Published on the web September 10, 2004; DOI 10.1246/bcsj.77.1741

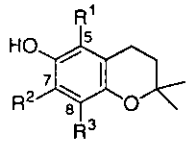

1H: $R^1 = R^2 = R^3 = CH_3$
5-CD_3-**1H**: $R^1 = CD_3$, $R^2 = R^3 = CH_3$
7-CD_3-**1H**: $R^1 = R^3 = CH_3$, $R^2 = CD_3$
8-CD_3-**1H**: $R^1 = R^2 = CH_3$, $R^3 = CD_3$

Chart 1. Vitamin E models.

Experimental

Materials. 2,2,5,7,8-Pentamethylchroman-6-ol (**1H**) was purchased from Wako Pure Chemical Ind. Ltd., Japan. 2,2-Bis(4-*tert*-octylphenyl)-1-picrylhydrazyl radical (DOPPH•) was obtained commercially from Aldrich. $Mg(ClO_4)_2$ and acetonitrile (MeCN; spectral grade) were purchased from Nacalai Tesque, Inc., Japan, and used as received. Three deuterated isotopomers (>98% isotopic purity) of **1H**, 5-CD_3-**1H**, 7-CD_3-**1H**, and 8-CD_3-**1H**, were synthesized according to the literature procedures.[30]

Spectral Measurements. A continuous flow of Ar gas was bubbled through a MeCN solution (3.0 mL) containing DOPPH• (1.4×10^{-5} M) (1 M = 1 mol dm^{-3}) in a square quartz cuvette (10 mm i.d.) with a glass tube neck for 10 min. The neck of the cuvette was sealed to ensure that air would not leak into the cuvette by using a rubber septum. A microsyringe was used to inject **1H** (2.0×10^{-2} M), which was also deaerated, into the cuvette. This led to a hydrogen-transfer reaction from **1H** to DOPPH•. UV–vis spectral changes associated with this reaction were monitored using an Agilent 8453 photodiode array spectrophotometer.

EPR Measurements. Typically, an aliquot of a stock solution of **1H** (1.0×10^{-3} M) was added to LABOTEC LLC-04B EPR sample tube containing a deaerated MeCN solution of DOPPH• (1.0×10^{-3} M) in the presence or absence of 0.1 M $Mg(ClO_4)_2$ under an atmospheric pressure of Ar. The EPR spectra of the phenoxyl radical **1•** produced in the reaction between **1H** and DOPPH• were taken on a JEOL X-band spectrometer (JES-RE1-XE). The EPR spectra were recorded under nonsaturating microwave power conditions. The magnitude of modulation was chosen so as to optimize the resolution and the signal-to-noise (S/N) ratio of the observed spectra. The g values and the hyperfine splitting constants were calibrated with a Mn^{2+} marker. A computer simulation of the EPR spectra was carried out using the Calleo ESR Version 1.2 program (Calleo Scientific Publisher) on an Apple Macintosh personal computer.

Results and Discussion

Upon the addition of vitamin E model **1H** to an acetonitrile (MeCN) solution of DOPPH•, the absorption band due to DOPPH• ($\lambda_{max} = 543$ nm) decreased, accompanied by an increase in the absorption bands at 402 and 423 nm due to the phenoxyl radidal **1•** with clear isosbestic points at 343, 374, and 437 nm. The absorption bands around 400 nm are typical for phenoxyl radical species of α-tocopherol.[5,31] Thus, this spectral change is ascribed to a hydrogen transfer from **1H** to DOPPH• to produce **1•** and hydrogenated DOPPH• ($DOPPH_2$) (Scheme 1). In fact, the characteristic EPR spectrum due to **1•** having a g value of 2.0047 was observed in the reaction of **1H** with DOPPH• in deaerated MeCN at 298 K, as shown in Fig. 1(a), although the observed EPR signal gradually decreased because of the disproportionation of **1•**, even in the absence of O_2.[5] The hyperfine coupling constants (hfc) of the observed EPR spectrum of **1•** were determined by a comparison of the observed spectrum with the computer-simulated spectrum, as shown in Fig. 1(a); the thus-obtained hfc values were assigned as listed in Table 1.[24,32,33]

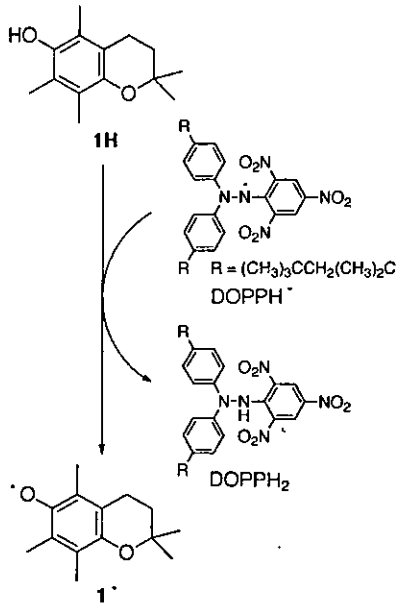

Scheme 1. Hydrogen transfer from **1H** to DOPPH• to produce **1•**.

On the other hand, in the presence of $Mg(ClO_4)_2$ (0.1 M), the absorption bands due to **1•** were shifted from 402 and 423 nm to 412 and 437 nm, respectively.[24] Such a red shift of the absorption bands indicates a complex formation between Mg^{2+} and **1•**. The EPR spectrum of the Mg^{2+}–**1•** complex was observed at $g = 2.0040$ [Fig. 1(b)], which is appreciably smaller than the g value of **1•** (2.0047), indicating that the spin density on oxygen nuclei in **1•** in the presence of Mg^{2+} is decreased by complexation with Mg^{2+}.[34] It should be noted that no decay of the EPR signal was observed, significantly demonstrating the enhanced stability of the phenoxyl radical species in the presence of $Mg(ClO_4)_2$.[24] This behavior is similar to that found for the α-tocopheroxyl radical in the presence of a fluorinated alcohol, which acts as a hydrogen-bond donor, by Lucarini et al.[35] The hyperfine structure can be reproduced by a computer simulation with the hyperfine coupling constants (hfc) of only two sets of methyl protons (0.486 and 0.335 mT), as shown in Fig. 1(b). However, the hfc values of the methylene protons and the remaining methyl protons become undetectably small. Since there are three methyl groups in the **1•** molecule, the assignment of these two hfc values due to two sets of methyl protons is quite complex.

In order to assign these hfc values obtained for the Mg^{2+}–**1•** complex, we synthesized three deuterated isotopomers of **1•**, i.e., 5-CD_3-**1•**, 7-CD_3-**1•**, and 8-CD_3-**1•**, where the methyl group at the C-5, C-7, or C-8 potision is replaced by the CD_3 group, respectively (Chart 1),[30] since deuterium substitution at appropriate known sites in the molecule permits an experimental verification of the assignment of the observed radical species (vide supra). A single deuteron gives a triplet (instead of a doublet) hyperfine pattern and the deuteron splitting should decrease due to the magnetogyric ratio of a proton to a deuteron (0.153).[25–29] In fact, deuterium substitution of the methyl group at the C-5 position of the Mg^{2+}–**1•** complex resulted in a drastic change in the splitting pattern from the spec-

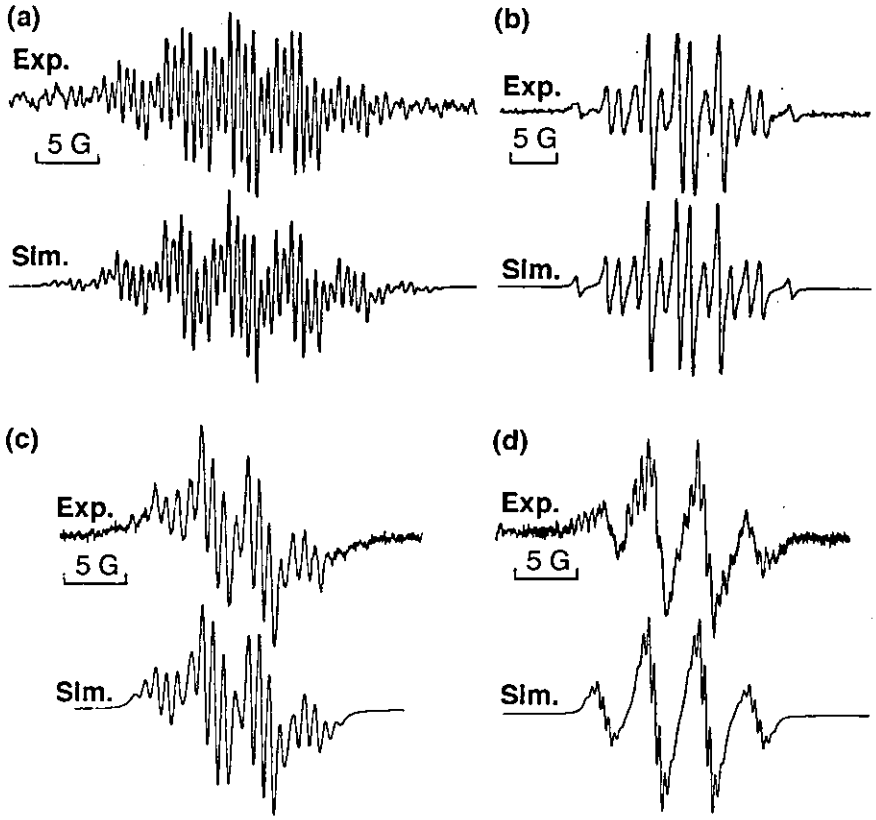

Fig. 1. EPR spectra of (a) **1**•, (b) Mg^{2+}–**1**•, (c) Mg^{2+}-5-CD_3-**1**•, and (d) Mg^{2+}–7-CD_3-**1**• in deaerated MeCN at 298 K with the corresponding computer simulation spectra. The hfc values used for the simulation are listed in Table 1.

Table 1. Hyperfine Splitting Constants (hfc) (in mT) of **1**• and the Mg^{2+} Complexes of **1**• and Its Deuterated Radicals in Deaerated MeCN

Radical	$a(3H^5)$	$a(3H^7)$	$a(3H^8)$	$a(2H^4)$
1•	0.587	0.440	0.086	0.139
Mg^{2+}–**1**•	0.486	0.335	—[a]	—[a]
Mg^{2+}-5-CD_3-**1**•	0.075[b]	0.335	—[a]	—[a]
Mg^{2+}–7-CD_3-**1**•	0.486	0.052[b]	—[a]	—[a]
Mg^{2+}–8-CD_3-**1**•	0.486	0.335	—[a]	—[a]

a) Too small to be determined. b) Deuterium splitting value.

trum in Fig. 1(b) to that in Fig. 1(c) for the Mg^{2+}-5-CD_3-**1**• complex generated in the same way. The hfc value of 0.486 mT of the Mg^{2+}–**1**• complex is decreased by the factor of the magnetogyric ratio of proton to deuterium (0.153) to 0.075 mT due to the CD_3 deuterons at the C-5 position of the Mg^{2+}-5-CD_3-**1**• complex, while the other hfc value (0.335 mT) remains identical, as shown in Fig. 1(c) and Table 1. From such a decrease in the hfc value at the C-5 position by the deuterium substitution, was assigned the hfc value at the C-5 position of the Mg^{2+}–**1**• complex as 0.486 mT.

A change in the splitting pattern was also observed upon deuterium substitution of the methyl group at the C-7 position of the Mg^{2+}–**1**• complex, as shown in Fig. 1(d). The computer simulation spectrum using the same hfc value, except for the deuterium at the C-7 position, which are reduced by a factor of 0.153, agrees well with the observed EPR spectrum of the Mg^{2+}–7-CD_3-**1**• complex [Fig. 1(d)]. On the other hand, a deuterium substitution of the methyl protons at the C-8 position of Mg^{2+}–**1**• resulted in no change in the splitting pattern in the EPR spectrum of the Mg^{2+}–8-CD_3-**1**• complex, as compared to the Mg^{2+}–**1**• complex (data not shown). From the above results, the hfc values of the Mg^{2+}–**1**• complex were assigned as listed in Table 1. The hfc values due to the methyl protons at the C-5 (0.587 mT) and C-7 (0.440 mT) positions are significantly decreased by complexation with Mg^{2+} (0.486 and 0.335 mT, respectively). No hyperfine structure was observed due to the methylene protons at the C-4 position, as well as the methyl protons at the C-8 protons in the Mg^{2+}–**1**• complex. It is clearly shown that the spin densities on the aromatic ring in the Mg^{2+}–**1**• complex are significantly decreased by the coordination of Mg^{2+}. Thus, an unpaired electron in **1**• is significantly delocalized into Mg^{2+} by complexation between **1**• and Mg^{2+} via the phenolic O atom.

In conclusion, the deuterium substitutions of the methyl group in **1H** enabled us to assign the hfc values of **1**• in the presence of Mg^{2+} experimentally. The decreased spin densities on the benzene ring in **1**•, the smaller g value of the EPR spectrum of **1**•, and the red shift of the absorption bands of **1**• in the presence of Mg^{2+} indicate that Mg^{2+} coordinates to the phenoxyl radical **1**• via the phenolic O atom of **1**•. Such complex formation between **1**• and Mg^{2+} precludes the disproportionation of **1**•, leading to the enhanced stability of **1**•. We are in the process of further exploring the effect of metal ions on the stability of phenoxyl radicals derived from phenolic antioxidants with a catechol moiety, such as (+)-catechin and quercetin.

This work was partially supported by a Grant-in-Aid for Scientific Research Priority Area (No. 11228205) and a Grant-in-Aid for Young Scientist (B) (No. 15790032) from the Ministry of Education, Culture, Sports, Science and Technology.

References

1 L. J. Machlin, "Handbook of Vitamins, Second Edition, Revised and Expanded," ed by L. J. Machlin, Marcel Dekker, New York (1991), pp. 99–144.

2 C. K. Chow, *Free Radical Biol. Med.*, **11**, 215 (1991).

3 G. W. Burton and K. U. Ingold, *Acc. Chem. Res.*, **19**, 194 (1986).

4 S. V. Jovanovic, S. Steenken, M. Tosic, B. Marjanovic, and M. G. Simic, *J. Am. Chem. Soc.*, **116**, 4846 (1994).

5 V. W. Bowry and K. U. Ingold, *J. Org. Chem.*, **60**, 5456 (1995)

6 C. Suarna, D. C. Craig, K. J. Cross, and P. T. Southwell-Keely, *J. Org. Chem.*, **53**, 1281 (1988).

7 M. Matsuo, S. Matsumoto, and T. Ozawa, *Org. Magn. Reson.*, **21**, 261 (1983).

8 T. Doba, G. W. Burton, and K. U. Ingold, *J. Am. Chem. Soc.*, **105**, 6505 (1983).

9 G. W. Burton, T. Doba, E. Gaba, L. Hughes, F. L. Lree, L. Prasad, and K. U. Ingold, *J. Am. Chem. Soc.*, **107**, 7053 (1985).

10 S. Urano, S Yamanoi, Y. Hattori, and M. Matsuo, *Lipids*, **12**, 105 (1977).

11 W. A. Skinner and P. Alaupovic, *J. Org. Chem.*, **28**, 2854 (1963).

12 H. Meerwein, *Angew. Chem.*, **67**, 374 (1955).

13 K. Dimroth, W. Umbach, and H. Thomas, *Chem. Ber.*, **100**, 132 (1967).

14 P. D. Boyer, *J. Am. Chem. Soc.*, **73**, 733 (1951).

15 W. Dürckheimer and L. A. Cohen, *J. Am. Chem. Soc.*, **86**, 4388 (1964).

16 C. Martius and H. Eilingsfeld, *Liebigs Ann. Chem.*, **607**, 159 (1957).

17 W. A. Skinner and R. M. Parkhurst, *J. Org. Chem.*, **31**, 1248 (1966).

18 J. L. G. Nilsson, J. O. Branstad, and H. Sievertsson, *Acta Pharm. Suec.*, **5**, 509 (1968).

19 D. R. Nelan and C. D. Robeson, *J. Am. Chem. Soc.*, **84**, 2963 (1962).

20 M. Fujimaki, K. Kanamaru, T. Kurata, and O. Igarashi, *Agric. Biol. Chem.*, **34**, 1781 (1970).

21 V. L. Frampton, W. A. Skinner, P. Cambour, and P. S. Bailey, *J. Am. Chem. Soc.*, **82**, 4632 (1960).

22 F. M. Dean, K. B. Hindley, L. E. Houghton, and M. L. Robinson, *J. Chem. Soc., Perkin Trans. 1*, **1976**, 600.

23 Y. Nagata, C. Miyamoto, Y. Matsushima, and S. Matsumoto, *Chem. Pharm. Bull.*, **47**, 923 (1999).

24 I. Nakanishi, K. Fukuhara, T. Shimada, K. Ohkubo, Y. Iizuka, K. Inami, M. Mochizuki, S. Urano, S. Itoh, N. Miyata, and S. Fukuzumi, *J. Chem. Soc., Perkin Trans. 2*, **2002**, 1520.

25 J. E. Wertz and J. R. Bolton, "Electron Spin Resonance Elementary Theory and Practical Applications," McGraw-Hill, New York (1972).

26 S. Fukuzumi, Y. Tokuda, T. Kitano, T. Okamoto, and J. Otera, *J. Am. Chem. Soc.*, **115**, 8960 (1993).

27 I. Nakanishi, S. Itoh, and S. Fukuzumi, *Chem.—Eur. J.*, **5**, 2810 (1999).

28 S. Fukuzumi, O. Inada, and T. Suenobu, *J. Am. Chem. Soc.*, **124**, 14538 (2002).

29 S. Fukuzumi, O. Inada, and T. Suenobu, *J. Am. Chem. Soc.*, **125**, 4808 (2003).

30 T. Ozawa, A. Hanaki, S. Matsumoto, and M. Matsuo, *Biochim. Biophys. Acta*, **531**, 72 (1978).

31 K. Mukai, Y. Watanabe, and K. Ishizu, *Bull. Chem. Soc. Jpn.*, **59**, 2899 (1986).

32 K. Mukai, N. Tsuzuki, K. Ishizu, S. Ouchi, and K. Fukuzawa, *Chem. Phys. Lipids*, **29**, 129 (1981).

33 J. Tsuchiya, E. Niki, and Y. Kamiya, *Bull. Chem. Soc. Jpn.*, **56**, 229 (1983).

34 S. Itoh, H. Kumei, S. Nagatomo, T. Kitagawa, and S. Fukuzumi, *J. Am. Chem. Soc.*, **123**, 2165 (2001).

35 M. Lucarini, V. Mugnaini, G. F. Pedulli, and M. Guerra, *J. Am. Chem. Soc.*, **125**, 8318 (2003).

Available online at www.sciencedirect.com
SCIENCE DIRECT®
ELSEVIER
Mutation Research 547 (2004) 101–107
Fundamental and Molecular Mechanisms of Mutagenesis
www.elsevier.com/locate/molmut
Community address: www.elsevier.com/locate/mutres

Correlation of sister chromatid exchange formation through homologous recombination with ribonucleotide reductase inhibition

Atsuko Matsuoka [a,*], Cecilia Lundin [b], Fredrik Johansson [b], Margareta Sahlin [c], Kiyoshi Fukuhara [d], Britt-Marie Sjöberg [c], Dag Jenssen [b], Agneta Önfelt [b]

[a] *Division of Medical Devices, National Institute of Health Sciences, 1-18-1 Kamiyoga, Setagaya-ku, Tokyo 158-8501, Japan*
[b] *Department of Genetic and Cellular Toxicology, Stockholm University, S-106 91 Stockholm, Sweden*
[c] *Department of Molecular Biology and Functional Genomics, Stockholm University, S-106 91 Stockholm, Sweden*
[d] *Division of Organic Chemistry, National Institute of Health Sciences, 1-18-1 Kamiyoga, Setagaya-ku, Tokyo 158-8501, Japan*

Received 8 August 2003; received in revised form 20 November 2003; accepted 5 December 2003

Abstract

We conducted the recombination and sister chromatid exchange (SCE) assays with five chemicals (hydroxyurea (HU), resveratrol, 4-hydroxy-*trans*-stilbene, 3-hydroxy-*trans*-stilbene, and mitomycin C) in Chinese hamster cell line SPD8 V79 to confirm directly that SCE is a result of homologous recombination (HR). SPD8 has a partial duplication in exon 7 of the endogenous *hprt* gene and can revert to wild type by homologous recombination. All chemicals were positive in both assays except for 3-hydroxy-*trans*-stilbene, which was negative in both. HU, resveratrol, and 4-hydroxy-*trans*-stilbene were scavengers of the tyrosyl free radical of the R2 subunit of mammalian ribonucleotide reductase. Tyrosyl free radical scavengers disturb normal DNA replication, causing replication fork arrest. Mitomycin C is a DNA cross-linking agent that also causes replication fork arrest. The present study suggests that replication fork arrest, which is similar to the early phases of HR, leads to a high frequency of recombination, resulting in SCEs. The findings show that SCE may be mediated by HR.

Keywords: Sister chromatid exchange; Homologous recombination; Hypoxanthine-guanine phosphoribosyltransferase; Ribonucleotide reductase

1. Introduction

Sister chromatid exchanges (SCEs) are induced during DNA replication [1,2], and evidence suggests that they are formed during homologous recombination (HR) [2–4]. Sonoda et al. [3] showed that spontaneous and mitomycin C-induced SCE frequencies were reduced in chicken DT40 B cells lacking the key HR genes *RAD51* and *RAD54*, but not in *KU70*$^{-/-}$ cells defective in non-homologous DNA end joining. When a human *RAD51* gene was inserted, HR activity was restored and SCE levels returned to normal [3]. Other experiments have also suggested that SCE formation is mediated by HR [5–8].

Resveratrol and some of its synthesized derivatives are potent inducers of SCEs in Chinese hamster lung

* Corresponding author. Tel.: +81-3-3700-9264; fax: +81-3-3707-6950.
E-mail address: matsuoka@nihs.go.jp (A. Matsuoka).

0027-5107/$ - see front matter
doi:10.1016/j.mrfmmm.2003.12.002

fibroblast (CHL) cells [9,10]. The active moiety is the 4′-hydroxy group [10]. Resveratrol, like hydroxyurea (HU), inhibits ribonucleotide reductase (RNR), which is essential for formation of deoxyribonucleotides and, therefore, DNA synthesis [11,12]. It appears to act by replication fork arrest in SCE formation [2] and in the SPD8 V79 cell line, HR [13], which carries a duplication in the *hprt* locus that renders it insensitive to thioguanine [14]. Following HR and loss of the duplication, the cells regain wild-type sensitivity to thioguanine [15,16].

In this work, we investigated resveratrol and its derivatives in an attempt to learn the mechanisms by which they induce cytogenetic effects. We applied resveratrol and derivatives that had or did not have a 4′-hydroxy group, and compared their effects on (1) tyrosyl radical decay in the purified R2 subunit of mammalian RNR and (2) SCE and HR in the SPD8 cell line. The chemicals we used in the biological tests were HU, a selective inhibitor of RNR, and mitomycin C, an efficient inducer of SCEs. However, while HU stimulated HR, mitomycin C appeared to be much less efficient in this respect despite its pronounced effect on SCE. The results have clear implications for the links between RNR inhibition, SCE formation, and HR, and the role of the 4′-hydroxy group.

2. Materials and methods

2.1. Cells

The SPD8 cell line was maintained in Dulbecco's modified eagle medium (GIBCO 11885-084) supplemented with 9% fetal bovine serum and penicillin-streptomycin (90 units/ml) (DMEM). 6-Thioguanine (5 μg/ml) was added to minimize the frequency of spontaneous reversion prior to treatment. The doubling time was around 12 h and the modal chromosome number was 22. SPD8 cells carry a duplication of exon 7 of the *hprt* gene and can be reverted by an exchange of Rad51-supported HR [16].

2.2. Chemicals

Resveratrol (CAS no. 501-36-0) purchased from Sigma Chemical Co. (St. Louis, MO, USA) and 3-hydroxy-*trans*-stilbene (17861-18-6) and 4-hydroxy-*trans*-stilbene (6554-98-9) synthesized as previously reported [17] were suspended homogeneously in physiological saline for the assays. Mitomycin C (MMC, 50-07-7) purchased from Kyowa Hakko Kogyo Co. Ltd. (Tokyo) was dissolved in distilled water and the solution was diluted with physiological saline. Hydroxyurea (HU, 127-07-1) purchased from Sigma was dissolved in physiological saline just before use. 6-Thioguanine (Sigma), hypoxanthine (Wako Pure Chemical Industries, Ltd. Osaka, Japan), and thymidine (Sigma) were first dissolved in as little 5 M sodium hydroxide as possible, then diluted with physiological saline and stored at −20 °C until use. L-Azaserine (Sigma) was dissolved in physiological saline and stored at −20 °C until use.

2.3. Recombination assay

Cells were seeded at a density of 1.0×10^6 20 ml DMEM/75 cm^2 flask, cultured for 4 h, and treated with a chemical for 20 h. Cells were rinsed, 20 ml DMEM was added, and the cells were allowed to recover for 30 h. We selected revertants by plating three dishes (3×10^5 cell/dish, 100 mm in diameter) in each treatment group and culturing them in the presence of HAsT (50 μM hypoxanthine, 10 μM L-azaserine, and 5 μM thymidine). Five hundred cells per dish were plated in duplicate for determination of the cloning efficiency. Seven days later, the colonies on the cloning plates were fixed with methanol and stained with Giemsa. The cells on the selection plates were also grown for 8 days, fixed, and stained. The reversion frequency was calculated as the total number of revertants on the selection plate divided by the total number of cells cloned at the same dose. The experiments were performed at least twice and representative data are shown.

2.4. Sister chromatid exchange assay

Cells were seeded at a density of 1.5×10^5 per plate (60 mm in diameter) and incubated for 17 h. The test chemical, then 5-bromodeoxyuridine (5 μM), was added, and the plate was incubated for 24 or 48 h. Chromosome preparations were made as follows: colcemid (final concentration 0.2 μg ml) was added

to the culture; 2 h later, the cells were trypsinized, incubated in hypotonic solution for 20 min at room temperature, and fixed three times with ice-cold fixative (glacial acetic acid: methanol, 1:3). A drop of the fixed cell suspension was placed on a clean glass slide and air-dried. A fluorescence-plus-Giemsa technique [18] was used for sister chromatid differentiation staining as previously reported [19]. SCEs were scored with the aid of a microscope in 25 second metaphase (M2) cells having 22 chromosomes at 600× magnification. Centromeric SCEs were indistinguishable from centric twists and were not scored. Solvent-treated cells served as the negative control. We analyzed SCE data using the Mann-Whitney *U*-test (the normal, two-tailed version).

2.5. Expression and purification of protein R2 from mouse ribonucleotide reductase

Protein R2 from mouse RNR was prepared from overexpressing BL21(DE3)pLYs cells containing the native pETR2 plasmid [20]. The purified protein, which was essentially apoprotein, was reconstituted to form the iron-tyrosyl radical center.

2.6. Experimental setup for kinetics of tyrosyl decay with test chemicals

The R2 apoprotein, ca. 7 μM in 50 mM aerobic Tris, pH 7.6, was reactivated by the addition of anaerobic 7 mM ferrous ammonium sulfate-5 mM ascorbic acid, in 50 mM Tris, pH 7.6, to the cuvette to give ca. 22 μM iron. The recorded reconstituted spectrum constituted the start spectrum for incubation with the different chemicals. The iron radical center of R2 has absorption bands in the 300–430 nm region. The tyrosyl radical has an absorption maximum at 416 nm. We followed the decay of the tyrosyl radical upon addition of a test chemical by observing the decay at 416 nm. The spectra were recorded on a Perkin-Elmer lambda 2 spectrophotometer, either with consecutive scans or as kinetic traces at 416 nm. The protein R2 concentration was typically 7 μM and we used equimolar concentrations of the chemicals. Because of the insolubility of the test chemicals in water, we dissolved them in acetone (final concentration 1%) for the spectroscopic measurements.

3. Results

3.1. Cytogenetic and recombination assays

The spontaneous reversion frequency in the recombination assay and baseline SCE frequency were $1.72 \pm 0.54 \cdot 10^5$ cells ($n = 36$) and 6.4 ± 3.0 cell ($n = 200$), respectively. Fig. 1 shows the SCE frequency at various treatment times with the higher ratio of M2 to total cells presented.

HU, the positive control for the recombination assay, induced revertants in a concentration-dependent manner up to 0.2 mM. HU induced a statistically significant increase in SCE frequency with a concentration-response relationship. SCEs were observed at 0–0.05 mM in 24-h treatment and at 0.1 mM in 48-h treatment.

Resveratrol and 4-hydroxy-*trans*-stilbene were positive in both assays with clear concentration-response relationships. 3-Hydroxy-*trans*-stilbene was negative in both assays and induced no delay in the cell cycle.

HU, resveratrol, and 4-hydroxy-*trans*-stilbene showed humped curves in the recombination assay and an increase in reversion frequency at concentrations that induced SCEs. MMC, the positive control for SCE induction, induced SCEs and revertants concentration-dependently, but at a higher concentration range for the latter (Fig. 1).

While MMC showed the peak reversion frequency at concentrations that induced severe toxicity, the other positive chemicals showed it at concentrations where the cloning efficiency was around 50% (Table 1). HU, resveratrol, and 4-hydroxy-*trans*-stilbene caused cell cycle delay, and peak SCE frequencies were seen at 48 h. At higher concentrations than those shown in Table 1, no metaphase cells were seen even at 48 h.

3.2. Tyrosyl radical decay in R2 of RNR

Decay of the tyrosyl radical of the *Escherichia coli* R2 unit of RNR was unaffected by resveratrol (data not shown). The decay of tyrosyl radical of R2 from mouse during incubation with 7.2 μM with each of the test chemicals is shown in Fig. 2. Decay was fastest with 4-hydroxy-*trans*-stilbene (estimated half life ($t_{1/2}$), ca. 57 s). For resveratrol, a small increase in absorption at 416 nm was observed at the beginning of the incubation time, and after the

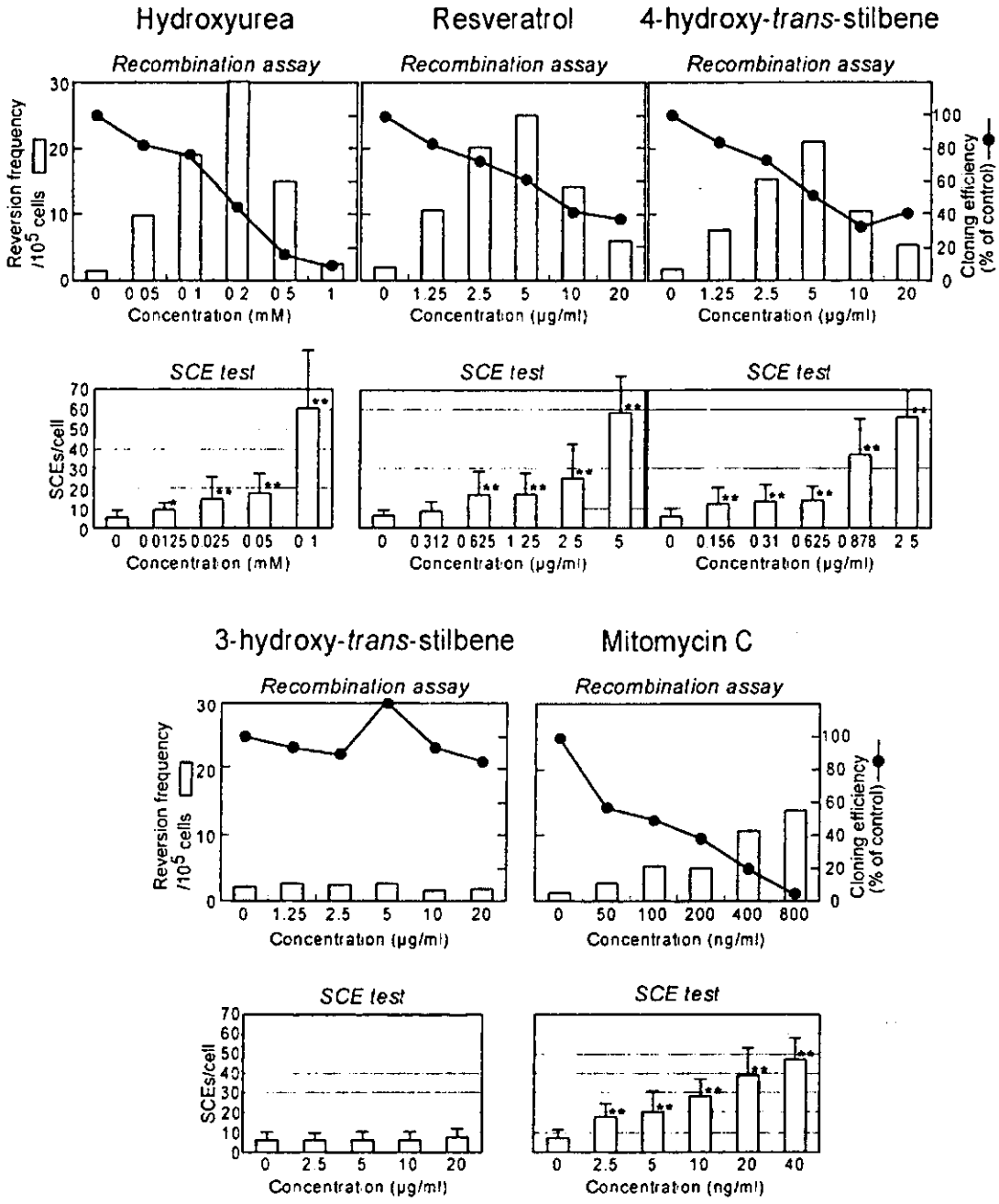

Fig. 1. Top: results of the recombination assay. The reversion frequency was calculated as the total number of revertants on the selection plate divided by the cloning efficiency at the same treatment concentration. Bottom: results of the SCE test in M2 cells ($n = 25$). Bars indicate S.D. $^{*}P < 0.001$, $^{**}P < 0.0001$.

Table 1
Toxicity of test chemicals at peak response in the recombination assay and the SCE test

	Recombination assay				SCE test			
	Concentration	Cloning efficiency (% of control)	Reversion frequency/10^5 cells	Ratio to[a] controls	Concentration	Treatment time (h)	SCEs/cell	Ratio to[a] controls
Hydroxyurea	0.2 mM	43	30.2	19.4	0.1 mM	48	60.9 ± 28.8	10.7
Resveratrol	5 μg/ml	60	25.1	11.8	5 μg/ml	48	58.7 ± 17.7	8.9
4-hydroxy-*trans*-stilbene	5 μg/ml	51	21.1	12.3	2.5 μg/ml	48	56.2 ± 13.1	9.6
Mitomycin C	400 ng/ml	19	10.7	8.3	40 ng/ml	24	47.5 ± 10.4	6.8
	800 ng/ml	3	13.9	10.8				

[a] Ratio to controls indicates the ratio of the reversion frequency or SCEs/cell to that of concurrent controls.

delay, the $t_{1/2}$ was ca. 67 s. At the lower concentrations of 4-hydroxy-*trans*-stilbene, we observed a similar increase in absorption prior to the onset of decay (data not shown). The increases may have been caused by the formation of a phenoxy-like radical in resveratrol and 4-hydroxy-*trans*-stilbene. Strikingly, 3-hydroxy-*trans*-stilbene did not cause decay of the tyrosyl radical.

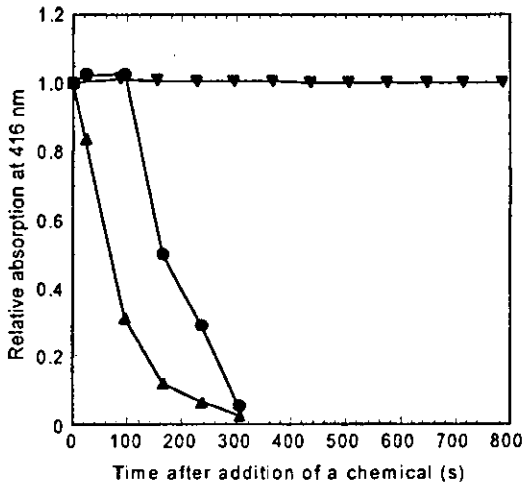

Fig. 2. Decay of tyrosyl radical of R2 protein of mouse ribonucleotide reductase. Solutions of R2 (7 μM) in 50 mM Tris buffer (pH 7.6) were incubated with 7.2 μM of resveratrol (●), 4-hydroxy-*trans*-stilbene (▲), or 3-hydroxy-*trans*-stilbene (▼). Spectra were recorded between 300 and 500 nm. Relative absorption at 416 nm (tyrosyl Abs_{max}) was calculated as relative absorption after subtraction of endpoint spectrum. Time 0 was set to 1.0 relative absorption. For 3-hydroxy-*trans*-stilbene no subtraction was performed since the tyrosyl radical did not decay.

4. Discussion

Micronucleus induction, SCE, mutation, and somatic recombination have been used to detect DNA damage and repair in genotoxic studies. These endpoints are usually applied independently, and they reflect different aspects of the repair processes. In the present study, we investigated the relationship between RNR-inhibition, SCE, and HR after exposure to five chemicals with different mode of action.

One of these, HU, scavenges the tyrosyl free radical in the R2 subunit of RNR, causing depletion of nucleotides [21,22] resulting in replication fork arrest [23]. The molecular conformation at the replication fork is similar to that at the recombination initiation site. That is, two DNA double strands of similar sequence align and a nick is formed in one of the strands. We suggest that the conformation may favor recombination, resulting in a high frequency of SCEs and HR.

Others have reported that resveratrol scavenges tyrosyl radicals of the R2 subunits from mice and *Arabidopsis thaliana* [12]. Here, we confirmed that observation in mice and showed that its analogue 4-hydroxy-*trans*-stilbene did the same while 3-hydroxy-*trans*-stilbene did not. HU, resveratrol, and 4-hydroxy-*trans*-stilbene caused HR and SCEs, while 3-hydroxy-*trans*-stilbene had no effect on either process. Thus, all these compounds should similarly induce RNR inhibition, SCE induction, and HR. Yet, the relationship between SCE and HR was complex. MMC, for example, which efficiently

induced SCEs was a poor inducer of HR via loss of the partial duplication. The response to very high and strongly cytotoxic concentrations suggests either a random effect coupled to survival, or another process facilitating HR. In any case, it appears that DNA damage leads into a pathway that stimulates SCE formation, but in some way prohibits the HR that leads to loss of the partial duplication and reversion to wild type. It remains to be investigated if this is coupled to less flexible conformations elicited by repair processes, possibly impairing the type of recombination required for reversion to wild type.

Using cytostatic drugs with different mode of action, Arnaudeau et al. [13] reported that inhibition of DNA synthesis induces HR in SPD8 cells. They used recombination indices (RIs) as an indicator of recombination potency. RI represents the ratio between the reversion frequency observed at a concentration associated with 50% cloning efficiency and the control reversion frequency. RIs of HU, resveratrol, 4-hydroxy-*trans*-stilbene, and MMC in the present study were 18, 9, 12, and 4, respectively. The RI of HU and MMC reported by Arnaudeau et al. [13] were close to ours, at 20 and 4, respectively. The findings suggest that recombination potency is related to the mechanism of action, as Arnaudeau et al. [13] noted.

At a concentration range where no metaphases were observed in the SCE test, reversion frequency of HU, resveratrol, 4-hydroxy-*trans*-stilbene decreased, indicating saturation of either the recombination machinery or the initiating event as shown in Fig. 1. HU induced structural chromosome aberrations in 10–30% of the cells at 0.1 and 0.2 mM, and resveratrol in 9–50% of the cells at 5 and 10 μg ml (SPD8 cells, data not shown). Thus, at higher concentrations, repair may not catch up with the increasing amount of DNA damage; many nicks may remain unrepaired, leading to chromosome aberrations in metaphase cells that escaped from S phase arrest.

In conclusion, all the chemicals induced both HR and SCE except for 3-hydroxy-*trans*-stilbene, which induced neither. We suggest that the observed correlation between tyrosyl radical decay in protein R2 of RNR and the frequency of HR and SCE support the view that SCE may be formed through HR during replication fork arrest.

Acknowledgements

This investigation was financially supported by the STINT (the Swedish Foundation for International Cooperation in Research and Higher Education) and the Swedish Cancer Foundation.

References

[1] S. Wolff, J. Bodycote, R.B. Painter, Sister chromatid exchanges induced in Chinese hamster cells by UV irradiation of different stages of the cell cycle: the necessity for cells to pass through S, Mutat. Res. 25 (1974) 73–81.
[2] H. Kato, Possible role of DNA synthesis in formation of sister chromatid exchanges, Nature 252 (1974) 739–741.
[3] E. Sonoda, M.S. Sasaki, C. Morrison, Y. Yamaguchi-Iwai, M. Takata, S. Takeda, Sister chromatid exchanges are mediated by homologous recombination in vertebrate cells, Mol. Cell. Biol. 19 (1999) 5166–5169.
[4] A. Kuzminov, Recombinational repair in eukaryotes, in: A. Kuzminov (Ed.), Recombinational Repair of DNA Damage, Springer-Verlag, New York, 1996, p. 185–203.
[5] A. Tutt, D. Bertwistle, J. Valentine, A. Gabriel, S. Swift, G. Ross, C. Griffin, J. Thacker, A. Ashworth, Mutation in Brca2 stimulates error-prone homology-directed repair of DNA double-strand breaks occurring between repeated sequences, EMBO J. 20 (2001) 4704–4716.
[6] M. Kraakman-van der Zwet, W.J.I. Overkamp, R.E.E. van Lange, J. Essers, A. van Duijn-Goedhart, I. Wiggers, S. Swaminathan, P.P.W. van Buul, A. Errami, R.T.L. Tan, N.G.J. Jaspers, S.K. Sharan, R. Kanaar, M.Z. Zdzienicka, Brca2 (XRCC11) deficiency results in radioresistant DNA synthesis and a higher frequency of spontaneous deletions, Mol. Cell. Biol. 22 (2002) 669–679.
[7] B.C. Godthelp, W.W. Wiegant, A. van Duijn-Goedhart, O.D. Schärer, P.P.W. van Buul, R. Kanaar, M.Z. Zdzienicka, Mammalian Rad51C contributes to DNA cross-link resistance, sister chromatid cohesion and genomic stability, Nucleic Acids Res. 30 (2002) 2172–2182.
[8] C.A. French, J.-Y. Masson, C.S. Griffin, P. O'Regan, S.C. West, J. Thacker, Role of mammalian RAD51L2 (RAD51C) in recombination and genetic stability, J. Biol. Chem. 277 (2002) 19322–19330.
[9] A. Matsuoka, A. Furuta, M. Ozaki, K. Fukuhara, N. Miyata, Resveratrol, a naturally occurring polyphenol, induces sister chromatid exchanges in a Chinese hamster lung (CHL) cell line, Mutat. Res. 494 (2001) 107–113.
[10] A. Matsuoka, K. Takeshita, A. Furuta, M. Ozaki, K. Fukuhara, N. Miyata, The 4′-hydroxy group is responsible for the in vitro cytogenetic activity of resveratrol, Mutat. Res. 521 (2002) 29–35.
[11] L. Thelander, P. Reichard, Reduction of ribonucleotides, Ann. Rev. Biochem. 48 (1979) 133–158.
[12] E. Elleingand, C. Gerez, S. Un, M. Knüpling, G. Lu, J. Salem, H. Rubin, S. Sauge-Merle, J.P. Laulhère, M. Fontecave,

Reactivity studies of the tyrosyl radical in ribonucleotide reductase from *Mycobacterium tuberculosis* and *Arabidopsis thaliana* Comparison with *Escherichia coli* and mouse, Eur. J. Biochem. 258 (1998) 485–490.

[13] C. Arnaudeau, E.T. Miranda, D. Jenssen, T. Helleday, Inhibition of DNA synthesis is a potent mechanism by which cytostatic drugs induce homologous recombination in mammalian cells, Mutat. Res. 461 (2000) 221–228.

[14] E. Dare, L.H. Zhang, D. Jenssen, Characterization of mutants involving partial exon duplications in the *hprt* gene of Chinese hamster V79 cells, Somat. Cell Mol. Genet. 22 (1996) 201–210.

[15] T. Helleday, C. Arnaudeau, D. Jenssen, A partial *HPRT* gene duplication generated by non-homologous recombination in V79 Chinese hamster cells is eliminated by homologous recombination, J. Mol. Biol. 279 (1998) 687–694.

[16] C. Arnaudeau, T. Helleday, D. Jenssen, The RAD51 protein supports homologous recombination by an exchange mechanism in mammalian cells, J. Mol. Biol. 289 (1999) 1231–1238.

[17] K. Thakkar, R.L. Geahlen, M. Cushman, Synthesis and protein-tyrosine kinase inhibitory activity of polyhydroxylated stilbene analogues of piceatanol, J. Med. Chem. 36 (1993) 2950–2955.

[18] P. Perry, S. Wolff, New Giemsa method for the differential staining of sister chromatids, Nature 251 (1974) 156–158.

[19] A. Matsuoka, M. Ozaki, K. Takeshita, H. Sakamoto, H.-R. Glatt, M. Hayashi, T. Sofuni, Aneuploidy induction by benzo[a]pyrene and polyploidy induction by 7,12-dimethylbenz[a]anthracene in Chinese hamster cell lines V79-MZ and V79, Mutagenesis 12 (1997) 365–372.

[20] U. Rova, A. Adrait, S. Potsch, A. Graslund, L. Thelander, Evidence by mutagenesis that Tyr (370) of the mouse ribonucleotide reductase R2 protein is the connecting link in the intersubunit radical transfer pathway, J. Biol. Chem. 274 (1999) 23746–23751.

[21] J.W. Yarbro, Mechanism of action of hydroxyurea, Semin. Oncol. 19 (1992) 1–10.

[22] S. Pötsch, M. Sahlin, Y. Langlier, A. Gräslund, G. Lassmann, Reduction of the tyrosyl radical and the iron center in protein R2 of ribonucleotide reductase from mouse, herpes simplex virus and *E. coli* by *p*-alkoxyphenols, FEBS Lett. 374 (1995) 95–99.

[23] L. Vassilev, G. Russev, Hydroxyurea treatment does not prevent initiation of DNA synthesis in Ehrlich as cites tumour cells and leads to the accumulation of short DNA fragments containing the replication origins, Biochem. Biophys. Acta. 781 (1984) 39–44

ITE Letters on Batteries, New Technologies & Medicine, Vol. 5, No. 6 (2004)

5 Water-Accelerated Radical-Scavenging Reaction of (+)-Catechin in an Aprotic Medium

Ikuo Nakanishi,[1,2,*] Tomonori Kawashima,[1,3] Kiyoshi Fukuhara,[4] Hideko Kanazawa,[3] Haruhiro Okuda,[4] Shunichi Fukuzumi,[2,*] Toshihiko Ozawa,[1] and Nobuo Ikota[1,*]

[1]*Redox Regulation Research Group, Research Center for Radiation Safety, National Institute of Radiological Sciences, Inage-ku, Chiba 263-8555, Japan*

[2]*Department of Material and Life Science, Graduate School of Engineering, Osaka University, CREST, Japan Science and Technology Agency (JST), Suita, Osaka 565-0871, Japan*

[3]*Department of Physical Pharmaceutical Chemistry, Kyoritsu University of Pharmacy, Minato-ku, Tokyo 105-8512, Japan*

[4]*Division of Organic Chemistry, National Institute of Health Sciences, Setagaya-ku, Tokyo 158-8501, Japan*

*Correspondence and requests for materials should be addressed to I.N. (E-mail: nakanis@nirs.go.jp; Fax: +81-43-255-6819).

Received October 13, 2004; accepted for publication October 15, 2004

ABSTRACT

The scavenging reaction of galvinoxyl radical ($GO^{\bullet}$) by (+)-catechin ($\mathbf{1H_2}$) in deaerated acetonitirile (MeCN), which is reported to proceed via an electron transfer from $\mathbf{1H_2}$ to $GO^{\bullet}$ to produce $\mathbf{1H_2}^{\bullet+}$ and GO^{-} followed by proton transfer, was significantly accelerated by the addition of H_2O. The strong solvation of H_2O to $\mathbf{1H_2}^{\bullet+}$ may result in the largely negative shift of the one-electron oxidation potential of $\mathbf{1H_2}$, resulting in the acceleration of the initial electron-transfer oxidation of $\mathbf{1H_2}$ by $GO^{\bullet}$.

KEYWORDS: Antioxidant; Oxidative stress; Catechin; Radical; Electron transfer; Water

INTRODUCTION

The mechanism of radical-scavenging reactions by phenolic antioxidants, such as polyphenols and tocopherols (vitamin E), has attracted considerable interest with regard to the development of novel chemopreventive agents against oxidative stress and associated diseases [1–3]. There are two mechanisms for the radical-scavenging reactions of phenolic antioxidants, i.e., a one-step hydrogen atom transfer from the phenolic OH group or an electron transfer followed by proton transfer [1–3]. Metal ions are a powerful tool to distinguish between these two mechanisms, since electron-transfer reactions are known to be significantly accelerated by the presence of metal ions [4]. In fact, we have recently reported that the scavenging reactions of the galvinoxyl radical ($GO^{\bullet}$) or cumylperoxyl radical ($PhMe_2COO^{\bullet}$) by (+)-catechin ($\mathbf{1H_2}$) (Fig. 1) in acetonitrile (MeCN) or in propionitrile, proceed via an electron transfer from $\mathbf{1H_2}$ to the radical, which was significantly accelerated by the presence of metal ions, such as Mg^{2+} and Sc^{3+}, followed by proton transfer [5,6]. In such a case, the coordination of metal ions to the one-electron reduced species of the radical may stabilize the product, resulting in the acceleration of the electron transfer [4]. These results suggest that polar solvents, such as water and alcohols, may stabilize the one-electron oxidized species of $\mathbf{1H_2}$ ($\mathbf{1H_2}^{\bullet+}$) via strong solvation to accelerate the electron-transfer process.

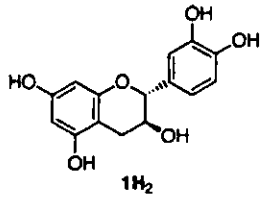

$\mathbf{1H_2}$

Fig. 1. Chemical structure of (+)-catechin ($\mathbf{1H_2}$).

We herein report that the scavenging-reaction of GO$^{\bullet}$ by (+)-catechin ($1H_2$) in deaerated MeCN is significantly accelerated by the addition of water. The results obtained in this study provide a valuable insight into the development of novel antioxidants with a more powerful radical-scavenging ability than natural-occurring ones.

MATERIALS AND METHODS

Materials

(+)-Catechin ($1H_2$) was purchased from Sigma and purified by column chromatography on silica gel using toluene/acetone/methanol as eluents with further recrystallization from *n*-hexane/ethyl acetate. The galvinoxyl radical (GO$^{\bullet}$) was commercially obtained from Aldrich. Acetoritirle (MeCN; spectral grade) was purchased from Nacalai Tesque, Inc., Japan, and used as received.

Kinetic measurements

Typically, an aliquot of (+)-catechin ($1H_2$; 2.0 × 10^{-2} M) in deaerated MeCN was added to a quartz cuvette (10 mm i.d.), which contained the galvinoxyl radical (GO$^{\bullet}$; 8.4 × 10^{-2} M) in deaerated MeCN (3.0 mL). UV–vis spectral changes associated with the reaction were monitored using an Agilent 8453 photodiode array spectrophotometer. The rates of the GO$^{\bullet}$-scavenging reactions by $1H_2$ were determined by monitoring the absorbance change at 428 nm due to GO$^{\bullet}$ (ε = 1.43 × 10^5 M^{-1} cm^{-1}) using a stopped-flow technique on a UNISOKU RSP-1000-02NM spectrophotometer. The pseudo-first-order rate constants were determined by a least-squares curve fit using an Apple Macintosh personal computer. The first-order plots of $\ln(A - A_\infty)$ vs. time (A and A_∞ are denoted as the absorbance at the reaction time and the final absorbance, respectively) were linear until three or more half-lives with the correlation coefficient $\rho >$ 0.999.

RESULTS AND DISCUSSION

Upon the addition of $1H_2$ to a deaerated MeCN solution of GO$^{\bullet}$, the absorption band at 428 nm due to GO$^{\bullet}$ immediately disappeared. This indicates that GO$^{\bullet}$ was efficiently scavenged by $1H_2$ via an electron transfer from $1H_2$ to GO$^{\bullet}$ to produce $1H_2^{\bullet+}$ and GO^{-}, followed by proton transfer [5,6]. The rates of the GO$^{\bullet}$-scavenging reaction by $1H_2$ were measured by monitoring the decrease in absorbance at 428 nm due to GO$^{\bullet}$ using a stopped-flow technique on a UNISOKU RSP-1000-02NM spectrophotometer. The decay of the absorbance at 428 nm due to GO$^{\bullet}$ obeyed pseudo-first-order kinetics when the concentration of $1H_2$ ($[1H_2]$) was maintained at more than a 10-fold excess of the GO$^{\bullet}$ concentration. The pseudo-first-order rate constants (k_{obs}) increase with the increasing $[1H_2]$ exhibited a first-order dependence on $[1H_2]$. From the slope of the linear plot of k_{obs} vs. $[1H_2]$, the second-order rate constant (k_{HT}) for the GO$^{\bullet}$-scavenging reaction by $1H_2$ was determined as 2.64 × 10 M^{-1} s^{-1} in deaerated MeCN at 298 K.

When H_2O is added to the $1H_2$–GO$^{\bullet}$ system, the rate of the GO$^{\bullet}$-scavenging reaction was significantly accelerated. The k_{HT} value linearly increases with the increasing H_2O concentration as shown in Fig. 2. Such an acceleration of the GO$^{\bullet}$-scavenging rates by H_2O may be explained by the strong solvation of H_2O with (+)-catechin radical cation ($1H_2^{\bullet+}$) generated in the initial electron transfer from $1H_2$ to GO$^{\bullet}$ as shown in Fig. 3. The complex formation of $1H_2$ and GO$^{\bullet}$ due to the strong solvation should result in the negative shift of the one-electron oxidation potential (E^0_{ox}) of $1H_2$, leading to a decrease in the free energy change of the electron transfer. The deprotonation of $1H_2$ may also be facilitated by H_2O. The E^0_{ox} value of $1H_2$ in MeCN containing H_2O could not be measured because of insolubility of the supporting electrolyte (Bu_4NClO_4) toward H_2O. However, the E^0_{ox} value of $1H_2$ in

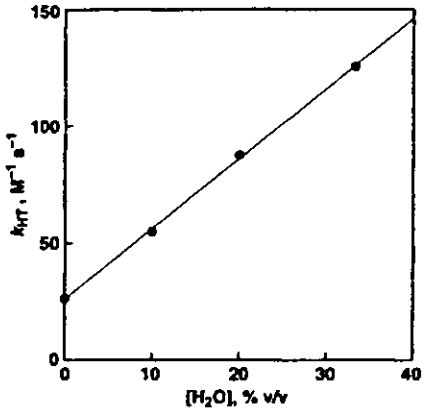

Fig. 2. Plot of k_{HT} vs. [H_2O] for the reaction of $1H_2$ with GO$^{\bullet}$ in deaerated MeCN/H_2O at 298 K.

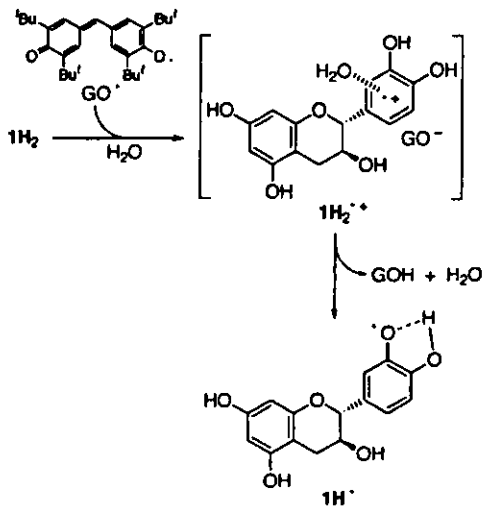

Fig. 3. Mechanism of water-accelerated GO·-scavenging by $\mathbf{1H_2}$.

methanol/phosphate buffer (0.1 M) (pH 7.5) (1:1 v/v) has been reported by flow-through electrolysis as 0.12V vs. SCE [7], which is significantly more negative than that in MeCN containing 0.1 M Bu_4NClO_4 (1.18 V vs. SCE [6]). A similar catalysis of H_2O has been observed for the multielectron oxidation of anthracene and its derivatives by one-electron oxidants, such as $[Ru(bpy)_3]^{3+}$ (bpy = 2,2'-bipyridine), where the water-accelerated electron-transfer disproportionation of the radical cations of the anthracenes occurs [8].

In conclusion, the GO·-scavenging ability of $\mathbf{1H_2}$ in deaerated MeCN is significantly enhanced in the presence of H_2O. The strong solvation of water to $\mathbf{1H_2}^{\cdot+}$ generated by the initial electron transfer from $\mathbf{1H_2}$ to GO· and the enhanced deprotonation of $\mathbf{1H_2}$ may result in the significant negative shift of the one-electron oxidation potential of $\mathbf{1H_2}$, leading to the acceleration of the reaction. The results obtained in this study suggest that the introduction of substituents, which can stabilize $\mathbf{1H_2}^{\cdot+}$, into $\mathbf{1H_2}$ may lead to the development of effective chemopreventive agents against oxidative stress and associated diseases.

ACKNOWLEDGMENTS

This work was partially supported by a Grant-in-Aid for Scientific Research Priority Area (No. 11228205) and a Grant-in-Aid for Young Scientist (B) (No. 15790032) from the Ministry of Education, Culture, Sports, Science and Technology, Japan.

REFERENCES

1. J. S. Wright, E. R. Johnson, and G. A. Di Labio. Predicting the activity of phenolic antioxidants: theoretical method, analysis of substituent effects, and application to major families of antioxidants. *J. Am. Chem. Soc.*, **123**, 1173-1183 (2001).
2. M. Leopoldini, T. Marino, N. Russo, and M. Toscano. Antioxidant properties of phenolic compounds: H-atom versus electron transfer mechanism. *J. Phys. Chem. A*, **108**, 4916-4922 (2004).
3. M. Leopoldini, I. P. Pitarch, N. Russo, and M. Toscano, Structure, conformation, and electronic properties of apigenin, luteolin, and taxifolin antioxidants. a first principle theoretical study. *J. Phys. Chem. A*, **108**, 92-96 (2004).
4. S. Fukuzumi, in *Electron Transfer in Chemistry*, ed. V. Balzani, Wiley-VCH, New York, 2001, Vol. 4, pp. 3-67.
5. I. Nakanishi, K. Miyazaki, T. Shimada, K. Ohkubo, S. Urano, N. Ikota, T. Ozawa, S. Fukuzumi, and K. Fukuhara. Effects of metal ions distinguishing between one-step hydrogen- and electron-transfer mechanisms for the radical-scavenging reaction of (+)-catechin. *J. Phys. Chem. A*, **106**, 11123-11126 (2002).
6. I. Nakanishi, K. Ohkubo, K. Miyazaki, W. Hakamata, S. Urano, T. Ozawa, H. Okuda, S. Fukuzumi, N. Ikota, and K. Fukuhara. A planar catechin analogue having a more negative oxidation potential than (+)-catechin as an electron transfer antioxidant against a peroxyl radical. *Chem. Res. Toxicol.*, **17**, 26-31 (2004).
7. B. Yang, A. Kotani, K. Arai, and F. Kusu. Relationship of electrochemical oxidation of catechins of their antioxidant activity in microsomal lipid peroxidation. *Chem. Pham. Bull.*, **49**, 747-751 (2001).
8. S. Fukuzumi, I. Nakanishi, and K. Tanaka. Multielectron oxidation of anthracenes with a one-electron oxidant via water-accelerated electron-transfer disproportionation of the radical cations as the rate-determining step. *J. Phys. Chem. A*, **103**, 11212-11220 (1999).

Ikuo Nakanishi, Researcher of Redox Regulation Research Group, National Institute of Radiological Sciences.
Areas: Physical chemistry for life science and electron-transfer chemistry.

Haruhiro Okuda, Director of Division of Organic Chemistry, National Institue of Health Sciences.
Areas: Bioorganic chemistry and regulatory science.

Tomonori Kawashima, Undergraduate student of Department of Physical Pharmaceutical Chemistry, Kyoritsu University of Pharmacy.
Areas: Physical pharmaceutical chemistry.

Shunichi Fukuzumi, Prof. of Department of Material and Life Science, Graduate School of Engineering, Osaka University.
Areas: Electron-transfer chemistry.

Kiyoshi Fukuhara, Section Chief of Division of Organic Chemistry, National Institute of Health Sciences.
Areas: Bioorganic chemistry and synthetic chemistry.

Toshihiko Ozawa, Executive Director of National Institute of Radiological Sciences.
Areas: Redox chemistry of reactive oxygens and free radicals; electron spin resonance application to biological systems.

Hideko Kanazawa, Prof. of Department of Physical Pharmaceutical Chemistry, Kyoritsu University of Pharmacy.
Areas: Physical pharmaceutical chemistry for analytical science and drug delivery system.

Nobuo Ikota, Director of Redox Regulation Research Group, National Institute of Radiological Sciences.
Areas: Synthetic organic chemistry and bioorganic chemistry.

A Planar Catechin Analogue Having a More Negative Oxidation Potential than (+)-Catechin as an Electron Transfer Antioxidant against a Peroxyl Radical

Ikuo Nakanishi,[†,‡] Kei Ohkubo,[†] Kentaro Miyazaki,[§,∥] Wataru Hakamata,[§] Shiro Urano,[∥] Toshihiko Ozawa,[†] Haruhiro Okuda,[§] Shunichi Fukuzumi,[*,‡] Nobuo Ikota,[*,†] and Kiyoshi Fukuhara[*,§]

Redox Regulation Research Group, Research Center for Radiation Safety, National Institute of Radiological Sciences, Inage-ku, Chiba 263-8555, Japan, Department of Material and Life Science, Graduate School of Engineering, Osaka University, CREST, Japan Science and Technology Agency, Suita, Osaka 565-0871, Japan, Division of Organic Chemistry, National Institute of Health Sciences, Setagaya-ku, Tokyo 158-8501, Japan, and Department of Applied Chemistry, Shibaura Institute of Technology, Minato-ku, Tokyo 108-8548, Japan

Received June 30, 2003

The hydrogen transfer reaction of antioxidative polyphenol with reactive oxygen species has proved to be the main mechanism for radical scavenging. The planar catechin (**P1H$_2$**), in which the catechol and chroman structure in (+)-catechin (**1H$_2$**) are constrained to be planar, undergoes efficient hydrogen atom transfer toward galvinoxyl radical, showing an enhanced protective effect against the oxidative DNA damage induced by the Fenton reaction. The present studies were undertaken to further characterize the radical scavenging ability of **P1H$_2$** in the reaction with cumylperoxyl radical, which is a model radical of lipid peroxyl radical for lipid peroxidation. The kinetics of hydrogen transfer from catechins to cumylperoxyl radical has been examined in propionitrile at low temperature with use of ESR, showing that the rate of hydrogen transfer from **P1H$_2$** is significantly faster than that from **1H$_2$**. The rate was also accelerated by the presence of Sc(OSO$_2$CF$_3$)$_3$. Such an acceleration effect of metal ion indicates that the hydrogen transfer reaction proceeds via metal ion promoted electron transfer from **P1H$_2$** to oxyl radical followed by proton transfer rather than via a one step hydrogen atom transfer. The electrochemical ease of **P1H$_2$** for the one electron oxidation investigated by second harmonic alternating current voltammetry strongly supports the two step mechanism for hydrogen transfer, resulting in the enhanced radical scavenging ability.

Introduction

Recently, much attention has been directed to the possibility of natural antioxidants, such as flavonoids, vitamin C, vitamin E, and β-carotene, as chemopreventive agents against oxidative stress and associated diseases (*1*−*3*). The generation of free radicals, such as hydroxyl radical ($^{\bullet}$OH) and superoxide anion ($O_2^{\bullet-}$), in biological systems is regarded as an important event contributing to the oxidative stress phenomena and one associated with many diseases, e.g., inflammentation, heart disease, cancer, and Alzheimer's (*4*−*6*). Flavonoids are plant phenolic compounds, which are widely distributed in foods and beverages and are extensively studied for their antioxidative and cytoprotective properties in various biological models (*7*−*9*). The antioxidative effects of flavonoids are believed to come from their inhibition of free radical processes in cells at three different levels: an initiation, by scavenging of $O_2^{\bullet-}$ (*10*, *11*); lipid peroxidation, by reaction with peroxyl or lipid peroxyl radicals (*12*); and the formation of $^{\bullet}$OH, probably by chelating iron ions (*13*). Besides their beneficial effects, there is also considerable evidence that flavonoids themselves are mutagenic (*14*, *15*) or carcinogenic (*16*) and show DNA damaging activity (*17*, *18*). Quercetin is a typical flavonoid that has been investigated as a potential chemopreventive agent against certain carcinogens (*19*, *20*). The chemistry of quercetin is predictive of its free radical scavenging ability. However, in biological systems, it was clearly demonstrated that quercetin could behave as both antioxidant and prooxidant. That is, dietary administration of excess quercetin induced renal tubule adenomas and adenocarcinomas in male rats (*21*) and induced intestinal and bladder cancer in rats (*22*). As other polyphenolic compounds, flavonoids may not show the sufficient antioxidative effects into the cells because of their hydrophilic properties, which impede the cell membrane translocation step (*23*). Therefore, much consideration to the safety should be required, when a large quantity of flavonoid is used as medicine for cancer chemoprevention.

In addition to the studies of natural antioxidants used for cancer chemoprevention or nutrition supplements, development of novel antioxidants that show improved radical scavenging activities has attracted considerable interest to remove reactive oxygen species (ROS), such as $O_2^{\bullet-}$ and $^{\bullet}$OH (*24*). We have previously reported that a planar catechin derivative (**P1H$_2$**) (Figure 1), synthesized in the reaction of (+)-catechin (**1H$_2$**) with acetone

* To whom correspondence should be addressed. Tel: 81-3-3700-1141. Fax: 81-3-3707-6950. E-mail: fukuhara@nibs.go.jp.
† National Institute of Radiological Sciences.
‡ Osaka University, CREST, Japan Science and Technology Agency.
§ National Institute of Health Sciences.
∥ Shibaura Institute of Technology.

10.1021/tx034134c CCC: $27.50
Published on Web 12/03/2003

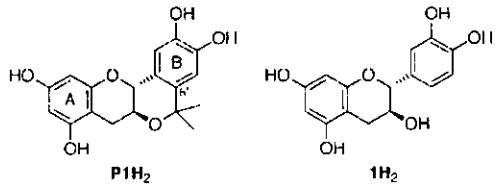

Figure 1. Chemical structures of planar catechin ($P1H_2$) and (+) catechin ($1H_2$).

in the presence of $BF_3{\cdot}Et_2O$ (*25, 26*), shows an enhanced protective effect against the oxidative DNA damage induced by the Fenton reaction without the prooxidant effect, which is usually observed in the case of $1H_2$. The spectroscopic and kinetic studies have demonstrated that the rate of hydrogen transfer from $P1H_2$ to galvinoxyl radical (G•), a stable oxygen centered radical, is about 5 fold faster than that of hydrogen transfer from the native $1H_2$ to G• (*26*). We have also demonstrated that the $O_2^{\bullet-}$ generating ability of the dianion form of $P1H_2$ generated in the reaction of $P1H_2$ with 2 equiv of Bu_4NOMe in deaerated acetonitrile (MeCN) is much lower than that of $1H_2$, suggesting that $P1H_2$ may be a promising novel antioxidant with reduced prooxidant activity (*27*). In addition, as compared with the hydrophilic $1H_2$, the lipophilic property of $P1H_2$, which is very soluble in alcohol, ether, and tetrahydrofuran, seems to give rise to its antioxidative activity into cell membrane.

We report herein that $P1H_2$ can also scavenge cumyl peroxyl radical ($PhCMe_2OO^{\bullet}$) more efficiently than $1H_2$. $PhCMe_2OO^{\bullet}$, while much less reactive than alkoxyl radicals, is known to follow the same pattern of relative reactivity with a variety of substrates (*28–30*). The effect of a metal ion on the rate of hydrogen transfer from $P1H_2$ to $PhCMe_2OO^{\bullet}$ was also examined in order to distinguish between the one step hydrogen atom transfer and the electron transfer mechanisms in the radical scavenging reaction of $P1H_2$ (*31*). The one electron oxidation potential (E_{ox}^{0}) of $1H_2$ as well as that of $P1H_2$ in MeCN was determined by the second harmonic alternating current voltammetry (SHACV). The combination of kinetic and electrochemical results obtained in this study provides confirmative bases to develop novel antioxidants that show improved radical scavenging activities.

Materials and Methods

Materials. A planar catechin derivative ($P1H_2$) was synthesized according to the literature procedure (*26*). (+) Catechin ($1H_2$) was purchased from Sigma. Di *tert* butyl peroxide was obtained from Nacalai Tesque Co., Ltd., and purified by chromatography through alumina, which removes traces of the hydroperoxide. Cumene was purchased from Wako Pure Chemical Industries Ltd., Japan. Tetra *n* butylammonium perchlorate (TBAP) used as a supporting electrolyte was recrystallized from ethanol and dried under vacuum at 313 K. MeCN and propionitrile (EtCN) used as solvent were purified and dried by the standard procedure (*32*).

Spectral and Kinetic Measurements. Kinetic measurements for the hydrogen transfer reactions between catechins and cumylperoxyl radical were performed on a JEOL X band spectrometer (JES ME LX) at 203 K. Typically, photoirradiation of an oxygen saturated EtCN solution containing di *tert* butyl peroxide (1.0 M) and cumene (1.0 M) with a 1000 W high pressure Mercury lamp resulted in formation of cumylperoxyl radical ($PhCMe_2OO^{\bullet}$; g = 2.0156), which could be detected at low temperatures. The g values were calibrated by using an Mn^{2+} marker. Upon cutting off the light, the decay of the ESR intensity was recorded with time. The decay rate was accelerated by the presence of $P1H_2$ (1.0×10^{-4} M). Rates of hydrogen transfer from $P1H_2$ to $PhCMe_2OO^{\bullet}$ were monitored by measuring the decay of the ESR signal of $PhCMe_2OO^{\bullet}$ in the presence of various concentrations of $P1H_2$ in EtCN at 203 K. Pseudo first order rate constants were determined by a least squares curve fit using an Apple Macintosh personal computer. The first order plots of $\ln(I - I_\infty)$ vs time (I and I_∞ are the ESR intensity at time t and the final intensity, respectively) were linear for three or more half lives with the correlation coefficient, $\rho > 0.99$. In each case, it was confirmed that the rate constants derived from at least five independent measurements agreed within an experimental error of 15%.

Scheme 1

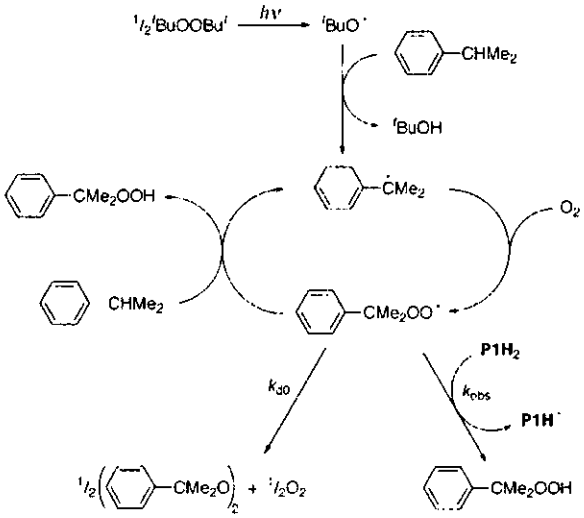

Electrochemical Measurements. The SHACV (*33–38*) measurements of $1H_2$ and $P1H_2$ were performed on an ALS 630A electrochemical analyzer in deaerated MeCN containing 0.10 M TBAP as a supporting electrolyte at 298 K. The platinum working electrode was polished with BAS polishing alumina suspension and rinsed with acetone before use. The counter electrode was platinum wire. The measured potentials were recorded with respect to an $Ag/AgNO_3$ (0.01 M) reference electrode. The one electron oxidation potentials (E_{ox}^{0}) (vs $Ag/AgNO_3$) were converted into those vs SCE by addition of 0.29 V (*39*).

Results

Hydrogen Transfer from Catechins to Cumylperoxyl Radical. Direct measurements of the rates of hydrogen transfer from a planar catechin derivative ($P1H_2$) to cumylperoxyl radical were performed in EtCN at 203 K by means of ESR. The photoirradiation of an oxygen saturated EtCN solution containing di *tert* butylperoxide (But^tOOBu^t) and cumene with a 1000 W high pressure mercury lamp results in formation of cumyl peroxyl radical ($PhCMe_2OO^{\bullet}$), which was readily detected by ESR. The cumylperoxyl radical is formed via a radical chain process shown in Scheme 1 (*40–44*).

The photoirradiation of But^tOOBu^t results in the homolytic cleavage of the O–O bond to produce $But^tO^{\bullet}$ (*45–51*), which abstracts a hydrogen from cumene to give cumyl radical, followed by the facile addition of oxygen to cumyl radical. The cumylperoxyl radical can also abstract a hydrogen atom from cumene in the propagation step to yield cumene hydroperoxide, accompanied by regeneration of cumyl radical (Scheme 1) (*52, 53*). In the termination step, cumylperoxyl radicals decay by a bimolecular reaction to yield the corresponding peroxide

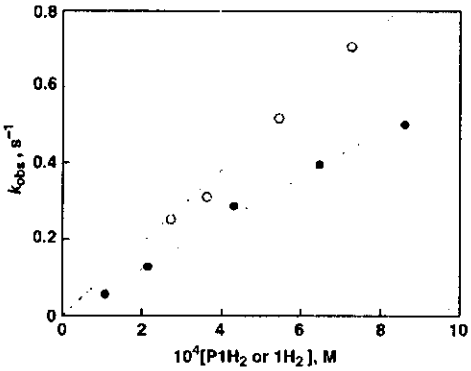

Figure 2. Plots of k_{obs} vs **P1H$_2$** (white circles) and vs **1H$_2$** (black circles) for the reactions of catechins (**P1H$_2$** and **1H$_2$**) with cumylperoxyl radical in EtCN at 203 K.

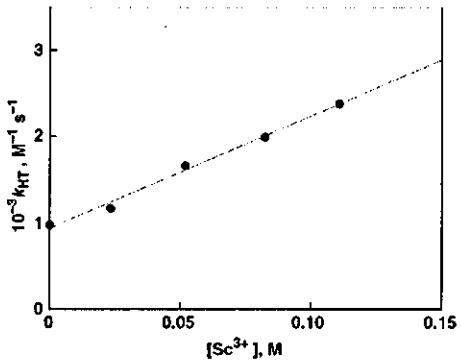

Figure 3. Plot of k_{HT} vs [Sc^{3+}] in the reaction of **P1H$_2$** to cumylperoxyl radical in the presence of $Sc(OSO_2CF_3)_3$ in EtCN at 203 K.

and oxygen (Scheme 1) (*41*, *42*). When the light is cut off, the ESR signal intensity decays obeying second order kinetics due to the bimolecular reaction in Scheme 1.

In the presence of **P1H$_2$**, however, the decay rate of cumylperoxyl radical after cutting off the light becomes much faster than that in the absence of **P1H$_2$**. The decay rate in the presence of **P1H$_2$** (1.0×10^{-4} M) obeys pseudo first order kinetics. This decay process is ascribed to hydrogen transfer from **P1H$_2$** to cumylperoxyl radical (Scheme 1). The pseudo first order rate constants increase with increasing **P1H$_2$** concentration ([**P1H$_2$**]) to exhibit first order dependence on [**P1H$_2$**] as shown in Figure 2. From the slope of the linear plot of k_{obs} vs concentration of **P1H$_2$** is determined the second order rate constant (k_{HT}) for the hydrogen transfer from **P1H$_2$** to cumylperoxyl radical as 9.7×10^2 M^{-1} s^{-1} in EtCN at 203 K.

Figure 2 also shows the linear plot of k_{obs} vs the concentration of (+) catechin (**1H$_2$**) for the reaction of **1H$_2$** with cumylperoxyl radical in EtCN at 203 K. The k_{HT} value for **1H$_2$** was also determined in the same manner as 6.0×10^2 M^{-1} s^{-1} (*31*). Thus, as in the case of galvinoxyl radical (*26*), the hydrogen transfer rate from **P1H$_2$** to cumylperoxyl radical is significantly faster than that from **1H$_2$**.

We have recently reported that the hydrogen transfer from **1H$_2$** to galvinoxyl or cumylperoxyl radical proceeds via electron transfer from **1H$_2$** to galvinoxyl or cumylperoxyl radical, which is accelerated by the presence of metal ions, such as Mg^{2+} and Sc^{3+}, followed by proton transfer (*31*). In such a case, the coordination of the metal ion to the one electron reduced species of galvinoxyl or cumylperoxyl radical may stabilize the product, resulting in acceleration of the electron transfer process. In this context, the effect of a metal ion on the k_{HT} value of **P1H$_2$** was examined. As in the case of **1H$_2$**, the hydrogen transfer from **P1H$_2$** to cumylperoxyl radical was significantly accelerated by the presence of $Sc(OSO_2CF_3)_3$ as shown in Figure 3. Thus, the hydrogen transfer from **P1H$_2$** to cumylperoxyl radical also proceeded via electron transfer from **P1H$_2$** to cumylperoxyl radical followed by proton transfer from **P1H$_2$**$^{\bullet+}$ to one electron reduced species cumylperoxyl radical as shown in Scheme 2.

The larger k_{HT} value of **P1H$_2$** as compared to that of **1H$_2$** may be ascribed to the stability of the radical cation of **P1H$_2$** (**P1H$_2$**$^{\bullet+}$), which is produced in the electron transfer from **P1H$_2$** to cumylperoxyl radical. The electron donating *i*-propyl group at the B ring of **P1H$_2$** may

Scheme 2

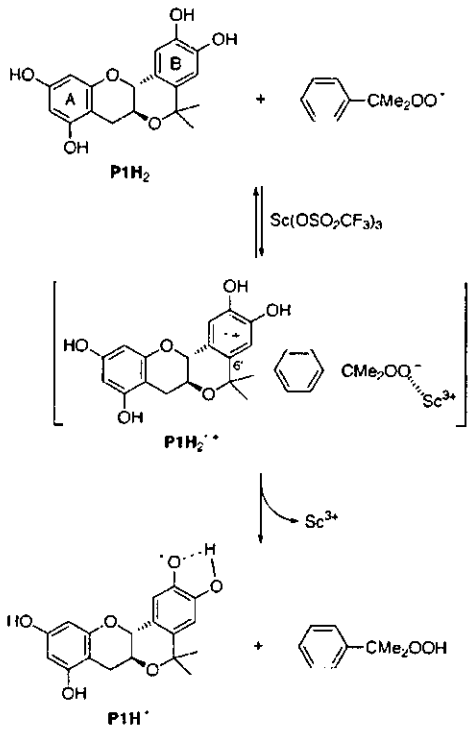

significantly stabilize **P1H$_2$**$^{\bullet+}$, resulting in the acceleration of the electron transfer step. In such a case, the one electron oxidation potential of **P1H$_2$** is expected to be more negative than that of **1H$_2$**.

One-Electron Oxidation Potential of a Planar Catechin Analogue. To determine the one electron oxidation potential of **P1H$_2$**, the cyclic voltammogram of **P1H$_2$** was recorded in MeCN containing 0.1 M TBAP as a supporting electrolyte at 298 K. Two irreversible oxidation (anodic) peaks were observed at 1.22 and 1.41 V vs SCE (data not shown). A similar cyclic voltammogram was obtained for **1H$_2$**, which exhibits irreversible oxidation peaks at 1.16 and 1.35 V vs SCE. This indicates that radical cations of **P1H$_2$** and **1H$_2$** are too unstable at the time scale of CV measurements. The SHACV method is known to provide a superior approach to directly evaluating one electron redox potential in the presence of the follow up chemical reaction relative to the better known dc and fundamental harmonic ac method (*34*). The